ISSN: 2994-6433

Research Article

Journal of Sensor Networks and Data Communications

Voronoi Structure of Space Integration with an Applied Roundabout Network – Part I

Ali Essam El-Shazly*

Department of Architectural Engineering, Fayoum University, Egyptc

***Corresponding Author:**
Ali Essam El-Shazly, Professor, Department of Architectural Engineering, Fayoum University, Egypt.

Submitted: 2024, Apr 19; **Accepted**: 2024, Jun 17: **Published**: 2024, Jul 08

Citation: El-Shazly, A. E. (2024). Voronoi Structure of Space Integration with an Applied Roundabout Network - Part I. *J Sen Net Data Comm, 4*(2), 01-16.

Abstract

The network objective of structuring space integration addresses the topologic and geometric dimensions to be framed out in a holistic method. In this sense, the spatial network of the multidisciplinary Voronoi convex hull encapsulates the varied integral properties with their correlative exploration. In practice, the conservation network of the roundabout Cairo investigates its integral structure against decomposition. The resultant structural essence defines the individual topological versus plural geometric roles at global integration per generator. The integrated topology cross-correlates control syntax with degree centrality in the local context, whereas the global structure of asymmetry complements the betweenness dynamics of generator distributiveness. Meanwhile, the geometrical network of the gabriel-graph forms cyclic spaces of global integrity and is correlated with Voronoi nodes at equidistant meeting points per cycle. Overlaid Voronoi properties classify the layout into clustered generators of correlated interval integrity, with functional cognition to infinity. An overview of the Voronoi network adopts intangible space integration along with its comprehensive framework of interrelated algorithms in the virtual reality of urbanism.

Keywords: Space Network, Voronoi Convex Hull, Topology, Geometry, Function, Integration

1. Introduction

The Napoleonic Expedition in Egypt in 1798 regenerated the Mediterranean culture of major transforms. One facet of cultural influence is occidental urbanism carried along imperial routes, sailing through the Suez shortcut. The universal city plan of the Haussmannization trend had first dazzled Cairo at the ceremonial time of inaugurating Suez in 1869 with worldwide monarchies invited. In this respect, the royalty requested the French engineer Haussmann in 1867 to design the Haussmannization of Cairo on his Parisian precedence of radial boulevards joining roundabouts at the Nile waterfront. The realized plan composed 15-roundabouts of superimposed boulevards overlapping with the pre-existing native town (Figs. 1 & 2). The building stock of neoclassical styles used to function for commercial, residential, administrative, and cultural activities to accommodate the mixed foreign community of continual increase. Over decades, Haussmann's foundation plan of Cairo had influenced the latter expansions up to total 153-roundabouts of radial boulevards towards satellite suburbs, with the core roundabouts defining Downtown Cairo and continuing to the present. However, the change after WW-II of socio-economic and cultural shifts has affected the roundabout-stock of vehicular priority [1].

The Researchers of modern Egyptian history refer to the massive twenty-volume document in 1889 entitled 'Khetat' or 'Plans,' which included the development of Haussmannized Cairo [2]. Nevertheless, the earlier Napoleonic Encyclopedia of 'Description De L'Egypte' stimulated the European modernization of Egypt [3]. Another distinctive archive in 1905 represents the 'Insurance Plan' of downtown Cairo and Alexandria, with full details on functional and ownership mapping [4]. The three documentaries portray Egypt in an unparalleled survey to enrich any library using extensive material on the status quo of modern Egypt with Haussmann's Cairo plan on top. Nevertheless, recent documents by M. Scharabi [5] and M. Volait [6] document the cultural values of special architecture in Downtown Cairo for conservation. In 2002, the Egyptian urban planning authority collaborated with Cairo University on the project of conserving Downtown Cairo, which

detailed the special merits of the area for visual enhancement [7]. Meanwhile, Haussmann's core 'Tahrir' roundabout had pinpointed the waves of national revolts until recent to become the symbolic memorial of future Egypt. Concurrent Conservation Act extends to the commemoration of Downtown Cairo for the universal identity of a democratic space [8]. This study continues to recognize the urban heritage of Downtown Cairo from the intangible scope of space structure and beyond tangible aspects [9]. In this regard, the cross-cultural foundation of roundabout geometry in Cairo crosses the visual borders into the invisible cognitive dimensions of virtual reality. In methodology, the virtual dimensions approach different but interrelated spatial structures of space syntax, shape grammar, GIScience, and Voronoi diagrams, which together funnel into the realm of artificial intelligence. The holistic convex space of the Voronoi diagram of algorithmic and mathematical dimensions was taken as the fundamental unit in methodological adaptation. The Voronoi convex hull of roundabout Cairo was processed and investigated according to the topological and geometric dimensions of 1) asymmetry and control, 2) Voronoi moments, and 3) Voronoi function, with their computational tools of programmable properties. The cross-correlation of Voronoi properties determines the cognitive structure of Cairo's roundabout network within a digital scope.

2. Methods

The rapid advancement of futurist GIScience has shifted human interaction from geographic location to cyberspace of topologic artificial intelligence and visual analytics [10]. The process of cyberspace includes spatiotemporal properties to embed in digital space, and thus the human interconnections in real geographical space and not only virtual reality [e.g., 11, 12, 13, 14]. The added visualization and sensing of cyberspace contribute to state-of-the-art GIScience dynamics such as meeting, shopping, trafficking, infrastructural, and pandemic monitoring along with multilayered digital datasets of smart and sustainable cities with their governance [15]. In the earlier practice of GIScience, the automation of space subdivision with database attribution and geometric modelling conceives the real world, in addition to the perceptual dimensions of humanities [e.g., 16, 17, 18]. The current practice extends the neural cognition of human-like robots in liveable geographic contexts that merge virtual reality with reality in cyberspace [e.g., 19, 20, 21, 22, 23]. In parallel, the artificial intelligence of computing architectural space flips the process from topologic space configuration to realizing geometrical forms of shape grammar [e.g., 24, 25, 26, 27, 28, 29]. Space syntax, in theory, is geometry-free according to the topological nature of social interactions in space in a logical layout [30]. The topology of a social network extends the syntax to the space isovist and configuration in a more shape-grammar approach on the rise [e.g., 31, 32, 33, 34, 35, 36] and GIScience as well [e.g., 37, 38]. In another computation, the non-visual Voronoi space of explicit tesselation defines a wider scope of implicit space that is interdisciplinary in nature, with extended applications of geometric and topologic objectives in common [39].

In mathematical terms, the digital space satisfies the geometric property of convexity for optimization and containment modeling [40]. Complex polyhedral geometry advances a new approach of full convexity in multidimensional space to resolve issues of connectedness [41]. The concept of 'convex space' structures the operational setting where informatics can be processed and linked to each other at different levels of resolution. The system of a 'convex hull' creates cellular extensions in space operators for undertaking digital interactions [e.g., 42, 43]. Diversity of space operators, nevertheless, structures the digital space according to the type of 'convex hull' for needed occupancy grid to overlay spatial data of geometric or topologic cognitive structure with their interrelationships [e.g., 44, 45]. In this regard, matching the type of convex hull with the applied dataset is the core issue in processing digital cognitive structures. In practice, shape grammar methodology is used to adopt a simple square box as the basic unit of spatial convexity [e.g., 46, 47, 48]. Later, the convex polyhedral was modeled as a bounding volume to process shape formation in a multidimensional space [e.g., 49, 50]. Recent developments have generated statistical rules for shape processing to overcome the descriptive design language of basic units with an imposed sequence of formal operations [51]. Meanwhile, the space syntax method adopts the convex space in a different manner of constructing contiguous space extensions in planar coordinates to form closed individual units of the largest possible convex spaces [30, p.97]. However, rules are applied in parallel to generate a spatial system according to the relationship between individual cells. Nevertheless, in GIScience, the convex space is applied in the wider mathematical scope of the smallest envelope for a set of points in the vector space [52]. The process of the Voronoi space is a representation of the convex hull in GIScience, where each point defines its convex boundaries relative to the others. Meanwhile, Voronoi individuality is another representation of the convex hull in space syntax, where each Voronoi point becomes the atom of convex space syntax [53]. Moreover, polyhedral representation as a Voronoi unit is another extension of shape grammar to create forms upon further descriptive or statistical ruling. In this regard, the standalone Voronoi space possesses a flexible interface to fit other concepts of spatial convexity in the digital scope. Investigating the virtual convex hull of the Voronoi space assumes fundamentality to other space structure methodologies with their associated geometric and topological cognition (Fig. 3).

3. Results

3.1. Voronoi Space

The two-way process of the Voronoi diagram tessellates the Euclidean plane into convex spaces of predefined generator points or locates the generator points from a predefined convex hull. The convex boundary line bisects the imaginary direct line joining each pair of generators if adjacent. Complete Voronoi edges shape the polygonal convex hull of first-order tesselation with the outer cells open to infinity. Applying the spatial process of Voronoi geometry to Haussmann's Cairo represents each of the total-15 roundabouts as a generator-point defining polygonal

premises (Figs. 4 & 5). The representation of a few generators may adopt the computer-aided design of CAD or GIS, whereas a larger generative system becomes more complicated and requires computational programming such as Wolfram [54]. In Wolfram's Mathematica program, Voronoi tesselation is simply obtained for any set of point processes in space as; DensityPlot[First[nf[{x, y}]], {x, -5, 5}, {y, -5, 5}, PlotPoints -> 100] [55]. The content of each convex polygon belongs to the generator roundabout at its geometric center. The resulting Voronoi convex hull enables a cross-comparative analysis among the planned generators in an extended scope of spatial measurements along topologic and geometric dimensions. The local control and global integral measures of topologic space syntax represent the basic statistical tools used to define the spatial structure in various convex maps. Meanwhile, each of the nonempty Voronoi polygons enriches the cognitive structure with informatics on function and urban tissues in relation to each other. The geometric Voronoi diagram adds further insights into moments such as distancing defined by the virtual fiber process of the Voronoi network. Cross-correlation of qualitative and quantitative Voronoi analyses recognizes the spatial structure of the roundabout Cairo in digital media.

The local measure of spatial control counts the ratio of adjacency of each Voronoi polygon in relation to its neighboring ones, where the higher the value, the more control the generator has over the surroundings (Table 1). The calculated control depends on the number of polygonal edges to exchange a portion of the total controlling amount over the vicinity in mutual but varying ratios with adjacent polygons [30, p.109]. The total value sums up the fractions received from adjacent generators, and thus, the control level of the polygonal generator. In common practice, the generator of control value above 'one' indicates a high level of spatial control. The measured control exhibited higher values of the inner polygons and decreased towards the boundary convex hull of the roundabout Cairo (Fig. 6). One distinctive exception is generator-12, which has the highest control at the boundary and among all others of the layout. Nevertheless, the classified control values exhibit three clusters of above-one, average-one, and below-one measures. The cluster above-one comprises generators 12, 9, 4, 15, and 6 in the control sequence. Although in a dispersed pattern, they form a continuous structure that spreads from one point adjacent to the other. Specific generator-4 demonstrates the core controller of the top-controlling generators in maximal attachment outwards. The cluster of average one corresponds to generators 10, 8, 14, 2, and 1 in the control order. Average control continues to occupy the inner polygons of the extended adjacency to the top-tier generators. The distribution forms an average buffer zone between the top and least control polygons during the transition. Nevertheless, the discrete pattern splits the average control into a continuous zone towards the Nile against the separated polygons inward. However, total discreteness forms a scattered pattern of the below-one control of the largest open polygons and the smallest enclosed cells. Therefore, the context of relative control measurement indicates a gradual shift from the highest to moderate zoning at the core convex hull with isolated open control.

Spatial integration extends the classified Voronoi convex hull into high, upper-medium, lower-medium and low integrity polygonal clusters (Fig. 7). The relative asymmetry (RA) measure of each Voronoi cell considers the depth of stepping adjacency to all other cells of the convex hull, with the lower RA value denoting a more integral space structure of the global layout system [30, p.108]. The top integration observes the innermost generators 4 & 9, which are also among the top controlling cluster in correlation. Meanwhile, the least layout integrity of generators 11, 13 & 7 coincides with the least control in another correlation as well. All inner bound polygons, nevertheless, are free from the least layout integrity of an inverse relationship to the least control pockets found. The moderate integration, however, forms two clusters of more integral generators towards the Nile edge and decreases at the opposite cluster of the convex hull. An overview of the layout integral structure forms concentric zones of optimum central integrity and lessens at outer rings. Further relationship observes generator-12 of upper-medium integrity without losing much credibility of being on top control. In another, generators 6 & 15 of lower-medium integrity have more contrast to their top-tier control. Similarly, generator-3 elevates from the least control cluster to upper-medium integration. Overlay of the local control context on the global layout integration is stable at top and bottom clustering of the convex hull, whereas the wider variation occurs at the moderate measurement of spatial structure. Also, the clusters of integral structure are more zoned up versus the scattered control pattern.

3.2. Voronoi Moments

The random point process of the roundabouts in the Euclidiean plane exerts various network moments of topological and geometric parameters such as centrality, Gabriel circle, and shape measurements of Voronoi analysis. The betweenness measure of centrality traces the network's geodesic shortest paths with the in-between encounters of each generator at the universal adjacency level of Voronoi polygons (Figs. 8-10 & Table 2). The more betweenness scored, the higher is the control or the cutting effect (or the critical integrity) of the generator's encounters over the global system. The resulted betweenness of Voronoi Cairo identifies generator-9 in top centrality of global shortest paths. Oppositely, generator-13 represents the least shortcut of 'zero' betweenness choice. The range, nevertheless, spans along four consecutive intervals of betweenness clusters. The top-tier is limited to generators 9 & 12 of wide variance from the following medium-high cluster. Despite its boundary setting, generator-12 boosts the betweenness apart from generator-9 to spread bipolar network of increased width of the convex hull structure. The medium-high interval spreads over polygons 4, 15 & 6 in sequence. The top-tier with generator-4 in between determines the critical zone of the global system to integrate. Meanwhile, generator-15 of direct adjacency to generator-9 revitalizes the peripheral convex

hull, whereas generator-6 adjacent to generator-4 maintains the same betweenness effect in a lesser tone though. Therefore, the two higher clusters of betweenness centrality decentralize the network integrity in maximum variety of innermost so as outermost choice along the Voronoi convex hull. Further medium-low of extended cluster forms a buffer zone between the highest and the remaining lowest betweenness. The latter exhibits a scattered pattern to diminish the effect of its low centrality on the overall betweenness scheme. The global context of clustered betweenness centrality coincides in total cross-correlation with the local context of spatial control towards cognitive structural blend.

Closeness centrality measures the depth efficiency of nodal connectivity at the global layout resolution. Generator-9 sustains on top and is followed by generator-4 in swap with the higher betweenness of generator-12, in addition to generator-2 of new entry to the highest clustering interval. In this regard, the closeness of generators 4 & 2 at efficient adjacency to the distinctive generator-9 gained more potential of layout centrality. The same two generators are adjacent to the other influential generator-12 in more efficiency, especially that of generator-4 surpassing the closeness centrality of generator-12 itself. The medium-high generators 10, 8 & 3 form a cluster adjacent to the top-tier closeness. Equal closeness of generators 3 & 8 differs in structure where the former is totally surrounded by the top-tier polygons compared to the latter of only generator-9 adjacency but more polygonal adjacencies in compensation. Meanwhile, the higher rank of generator-10 has equal adjacencies as of generator-8 with two instead of one top-tier connectivity of more privileged efficiency. Nevertheless, obscured judgment only by the degree of adjacency needs to expand the resolution of connectivity for justifying either idle or active closeness efficiency in propagation. Further cluster of medium-low closeness may clarify the matter where all generators are found sharing the same score. Three of them cluster around generator-8 of more justified efficiency, in addition to generator-10 adding one moderate-rank closeness (generator-15) to the previous highest ones. Therefore, the bigger picture resolution justifies the network of higher closeness centrality by virtue of spreading adjacencies and not only powerful direct connectivity as generator-3 proves. The cluster of the least closeness reaffirms the constant dissipation of generators 7, 11 & 13 of scattered pattern at the peripheral convex hull. Overview of clustered intervals disseminates their pattern in propagative rings from the core convex hull outwards. Meanwhile, the resulted closeness centrality pattern totally projects on the other pattern of spatial integration in complete cross-correlative phenomenon.

Degree centrality measures the polygonal extent of connectivity at the local context in standardized comparison to the global context of the convex hull. The interval clustering continues the same polygonal network structure with the same range from the top generator-9 to the bottom generator-13. The medium interval, however, floats in the widest exchange of structure to form the medium-high generators 15, 10, 8, 6 & 2 with the extended medium-low generators 14, 5, 3 & 1 of degree sequence. Here generator-15 regains its higher rank in degree as in betweenness but dropped in closeness, whereas generator-3 swaps the float in reverse. The narrow variance within clusters, nevertheless, limits the swapping impact on the global structure of stable centrality dimensions. Meanwhile, the degree centrality in particular extends to another crucial property of Gabriel-circle investigation. A circle is Gabriel if its diameter connecting the adjacent generators contains no other generator [39, p.97]. This property is verified for each of the generator's adjacencies, where it ends up synonymous with the Pitteway graph structure (Fig. 11). Exclusive relationships of adjacent generators maximize their proximity of cognitive structure on the global context. The resulted graph from the Gabriel circle property is highly cyclic where each generator shares a loop or more except generators 13 & 15 of only tail structure. The contraction of single-vertex tail sustains the global structure along complete cyclic space. Looping structure endorses the layout integrity from single Gabriel proximity into larger groups in a circle. In this regard, the global layout satisfies one large Gabriel cycle composed of smaller embedded ones at different levels of resolution. The largest ring encompasses the boundary convex hull along generators 14, 12, 1, 11, 10, 9, 8, 7, 6, 5, 4 and back to the start point. Minor cycles spread all over the convex hull with the possibility of merging at any resolution. The largest minor cycle composes generators 14, 12, 2, 3, & 4 in a large mix of previously clustered centrality. Specific generator-2 shares four-cycles at one point of layout maximal joint in correlation to its top-tier closeness centrality.

Moments of Voronoi fiber-process concerns the geometrical shaping of each polygon in terms of edge lengths, angles, area, perimeter, in addition to the property of triple-equidistance from adjacent generators to their shared Voronoi vertex (Fig. 12). The equidistance spot implies the imaginary 'meeting-point' of polygonal conjunction at the virtual space structure. Some Voronoi generators have shorter equidistance of stronger relationship than others, which transmutes the topologic measure of integration into a geometric moment. Setting the intervals of equidistance integrity classifies the mutual clusters of nearest, average, and farthest catchment area. Sets of nearest equidistance compose generators 5, 8, 9 & 6 among each other at one cluster versus generators 1, 2, 10 & 11 at the opposite discrete cluster. Farthest equidistance, nevertheless, of a kilometer relationship forms a southern cluster of generators 12, 13 & 14 and another discrete set of 10, 11 & 15 generators northwards. The moderate cluster has nearer links of generators 3, 9, 7, 6, 8, 4, 5, 2 & 10 and farther 12, 1, 2, 3, 15, 7, 8, 4 & 9 in cross-relationships among each other and among the extreme clusters as well. In this regard, each generator deploys integral equidistance at various classes of clustered adjacencies simultaneously. For example, generator-10 integrates equidistantly at nearest (1, 10, 11), moderate (2, 9, 10), and farthest (10, 11, 15) classes of diverse global clusters. The wide interval of moderate equidistance spreads all- around the layout in overlap with the extreme range of clusters, thus the versatile geometry of global integration. Meanwhile, the equidistance property set-in-train other geometrical moments of sorted out perimeter lengths, angling, and area

of Voronoi polygons in respective clusters. Overview of geometric equidistant integrity exceeds the cross-correlation of singular topologic role per generator by plural adjustments of global-wide clustering in network overlap.

3.3. Voronoi Function

Overlay of Voronoi convex hull on the historical plan of Cairo explores the function of virtual subdivision per polygon in details. The convex hull forms two functional zones of old and new Cairo in overlap at the border cells 12, 4 & 9 of effective control and integral space structure as measured. Key cells articulate 'Ezbekieh plaza, Nile promenade, Cairo Station, Cairo Citadel, Abdin palace, and Hippodrome' which correspond to polygons '6-7-8, 1-12-11, 15, 13, 3-4, 9' respectively. At the old Cairo zone, polygon-6 superimposes two commercial thoroughfares towards 'Azhar & Citadel' landmarks. Meanwhile, plolygon-7, projects another commercial spine up to Cairo Station with the 'Choubra' garden-city suburbs beyond. In this regard, least integral generators 13, 14 & 15 retreat direct links over the irregular pattern to integratelandmarks on the global city resolution with commercial synchronicity down to 'Ezbekieh' hub. The gardened hub itself extends new business offices, dwellings, and retails of new 'Okelle' building type of eclectic galleria-wekala traditions next to new landmarks such as foreign consulates and commune complexes, hotels, theaters, administrative facilities, in addition to the royal opera at generator-8 of exclusive drop-off. Nevertheless, new Cairo at the Nile frontier of gardened polygons developed royal palaces and prestigious housing of unbound polygons to infinity. Projecting the unbound edges over the Nile set generator-1 of 'Tahrir' to contain the Pyramids plateau with realized access along the Nile Bridge crossing to the Pyramids thoroughfare aided by tramline at Giza suburbs, thus the city assemblage in Voronoi network (Figs. 13-15). Overview of functional Voronoi polygons conform the virtual image of roundabout Cairo to be real districts, nodes, landmarks, paths, and edges at the global resolution of cognitive structure [56].

4. Discussion

Discussion of Voronoi's extended scope adds a new cognitive layer of intangible convex hull to the tangible aspects of space design, where geometric and topologic properties become virtually enabled. Parametric connectivity and distancing criteria of generated Voronoi polygons relate to each other at local and global contexts of layout structure. The spatial measurements aided by computing tools recognize the integral structure at different levels of resolution with overlay on the image of functional space. As for the case of Cairo, there is a geodesic evidence of Voronoi relationship that combines asymmetry and control of space syntax with the centrality structure of betweenness and closeness, though of different topology measures. Meanwhile, the standardized degree centrality allows the swap of ranking spaces per cluster without altering the global geodesic structure. The geometric space, nevertheless, restructures the global degree centrality into the Gabriel algorithm of paired adjacencies in circles of exclusive relationship. Tracking the geometric network of Gabriel graph shifts the Voronoi space into circuiting algorithms of artificial intelligence at the layout's global level. In this regard, the integral structure extends from topologic to geometric graph network connectivity. Nonetheless, the Voronoi's fiber-process itself is a dual geometric network where scaled moments project on the generative point process in space. The key property of equidistance ties the generators in triples at each Voronoi vertex with further integral structure explored at the global layout. In another, functional interaction along the convex hull of infinite Voronoi extents completes the recognition of space structure with the associated image attached to the cyber-space of visualized virtual reality. While this study is limited in scope, further prospects magnify the bigger-picture of virtual-real space structure in unlimited Voronoi application.

5. Conclusions

The applied prospect of Voronoi convex-hull encompasses topological and geometrical issues of space syntax, centrality, and graph algorithms towards a novelty framework of structuring space integration. The Voronoi embedment of multiple network dimensions enables the multilayered properties to be recognized and sieved in correlation to one another. Interconnected measurements of Voronoi space reveal the invisible structure per generator at different levels of integral resolutions with layout classification. The inferential application on any space at any scale retrieves the clustered integration with interpretational cognitive mapping. Proof by detailed Voronoi of Cairo's roundabout case concludes as follows (Table 3):

1. The topologic network of depth measure integrates the layout along three parameters of asymmetrical, betweenness, and closeness algorithms at global resolution of cross-comparison per network and among the collective networks as well. At Cairo, the clustered closeness centrality is observed correlating to the asymmetrical depth integrity whereas the global betweenness ties with both the local context of control measure and the global degree centrality. The topologic syntax, thus, set the asymmetric distributiveness along the closeness network of influential depth connectivity, but the shortest-path betweenness follows the control structure at both local degree context and the globally standardized centrality. Each network, nevertheless, diversifies the clustering structure along plural generators of maximized choice to limit the effect of cutting-vertices amid sustainable layout integrity.
2. The geometric network of Gabriel and equidistant moments extend the parameter of circular pairing-up of generators from the local context towards the global resolution of Gabriel graph algorithm, while equating the assembly of generators at the Voronoi corners. The Gabriel graph of Cairo enhances the integral layout structure of encircled minor circles at one major circle. The embedded looping spaces, thus, maximize the integral distributiveness at various lengths of circuiting extents per generator. Meanwhile, the equidistance property adjusts single generators at plural meeting points with multiple groups of generators at various extents in overlap. Therefore, the scaled geometry of generators satisfies the globally integrated layout at various extents of looping and distancing

resolutions of plural space structure per generator in contrast to the single strategy of generator topology but of multi-width.

3. Clustered generators classify the integral structure per generator in vertical cross-section of topologic-geometric networks. Top-tier integral class identifies generators 9, 12 & 4 of colorful encounters by the network parameters. This is followed in overlap of the middle-high class by generators 2, 10, 8 & 3 then the middle-low generators 1, 5, 6 & 14 in sequence. Constant low integral class set generators 13, 11 & 7 apart. Projecting the classified clusters on the cognitive structure of roundabout Cairo set the highest layout integrity at the core zone of Voronoi convex hull whereas the moderate integrity shares the two opposite poles at the waterfronts of the Nile and Ezbekieh Lake with the high core zone at an in-between logic. The least integrity occurs for a reason to buffer the bulk of workshops at polygon-11 extent and the least found landmarks to integrate in generator-7, in addition to Cairo Citadel of visual overwhelm from top and not network integrity. The networking of generator-15, however, has equally distributed structure along the classified tiers thus the spanning integral strategy of Cairo Station depot.

Declaration of Interests

The research paper declares to have no known competing financial interests or personal relationships that could have appeared to influence the work reported.

References

1. El-Shazly, A. E. (2003). The Prospects of the 'European Quarter'in Cairo. *Journal of Asian Architecture and Building Engineering, 2*(1), 175-182.
2. Mubarak, A. (1889). Khetat. Beaulac Press, Cairo. (In Arabic)
3. Neret, G. (2001). Description de L'Egypte, Taschen. (Originally published by the French Imperial Press in 1802)
4. El Shazly, A. E. (2019). The Future of the 'Insurance Plan'in Cairo and Alexandria. In *Conservation of Architectural Heritage: A Culmination of Selected Research Papers from the Second International Conference on Conservation of Architectural Heritage (CAH-2), Egypt 2018* (pp. 9-22). Springer International Publishing.
5. Scharabi, M. (1989). *Kairo: stadt und architektur im zeitalter des europäischen kolonialismus.* Wasmuth.
6. Volait, M. (2001). *Le Caire, Alexandrie, Architectures européennes, 1850-1950.* Presses de l'IFAO.
7. The Town Planning Department and Cairo University (2002). The European Quarter of Cairo: A Study in conservation, Final Report, Published by the Town Planning Department, Cairo.
8. Attia, S. (2012). Revitalization of Downtown as center for social democracy and sustainable growth. *Ecocity Summit Book Library.*
9. El Shazly, A. E. (2019). On the Spatial Conservation of Roundabout Cairo Using Pitteway Graph. In *Conservation of Architectural Heritage: A Culmination of Selected Research Papers from the Second International Conference on Conservation of Architectural Heritage (CAH-2), Egypt 2018* (pp. 23-36). Springer International Publishing.
10. Chen, M., Claramunt, C., Çöltekin, A., Liu, X., Peng, P., Robinson, A. C., ... & Lü, G. (2023). Artificial intelligence and visual analytics in geographical space and cyberspace: Research opportunities and challenges. *Earth-Science Reviews, 241,* 104438.
11. Han, S. Y., Tsou, M. H., & Clarke, K. C. (2018). Revisiting the death of geography in the era of Big Data: The friction of distance in cyberspace and real space. *International Journal of Digital Earth, 11*(5), 451-469.
12. Mohebbi, S., Zhang, Q., Wells, E. C., Zhao, T., Nguyen, H., Li, M., ... & Ou, X. (2020). Cyber-physical-social interdependencies and organizational resilience: A review of water, transportation, and cyber infrastructure systems and processes. *Sustainable Cities and Society, 62,* 102327.
13. Gao, C., Guo, Q., Jiang, D., Wang, Z., Fang, C., & Hao, M. (2019). Theoretical basis and technical methods of cyberspace geography. *Journal of Geographical Sciences, 29*, 1949-1964.
14. Batty, M. (1997). Virtual geography. *Futures, 29*(4-5), 337-352.
15. Xing, J., Sieber, R., & Roche, S. (2020). Rethinking spatial tessellation in an era of the Smart City. *Annals of the American Association of Geographers, 110*(2), 399-407.
16. Goodchild, M. (2010). Twenty years of progress: GIScience in 2010. *Journal of spatial information science,* (1), 3-20.
17. Winter, S., & Freksa, C. (2012). Approaching the notion of place by contrast. *Journal of Spatial Information Science,* (5), 31-50.
18. Luo, W., & MacEachren, A. M. (2014). Geo-social visual analytics. *Journal of spatial information science, 2014*(8), 27-66.
19. Zhang, Z., Qian, Z., Zhong, T., Chen, M., Zhang, K., Yang, Y., ... & Yan, J. (2022). Vectorized rooftop area data for 90 cities in China. *Scientific Data, 9*(1), 66.
20. Zhang, K., Qian, Z., Yang, Y., Chen, M., Zhong, T., Zhu, R., ... & Yan, J. (2022). Using street view images to identify road noise barriers with ensemble classification model and geospatial analysis. *Sustainable cities and society, 78,* 103598.
21. Qian, Z., Chen, M., Zhong, T., Zhang, F., Zhu, R., Zhang, Z., ... & Lü, G. (2022). Deep Roof Refiner: A detail-oriented deep learning network for refined delineation of roof structure lines using satellite imagery. *International Journal of Applied Earth Observation and Geoinformation, 107*, 102680.
22. Qian, Z., Chen, M., Yang, Y., Zhong, T., Zhang, F., Zhu, R., ... & Yan, J. (2022). Vectorized dataset of roadside noise barriers in China using street view imagery. *Earth System Science Data, 14*(9), 4057-4076.
23. You, L., Guan, Z., Li, N., Zhang, J., Cui, H., Claramunt, C., & Cao, R. (2021). A spatio-temporal schedule-based neural network for urban taxi waiting time prediction. *ISPRS International Journal of Geo-Information, 10*(10), 703.
24. Haakonsen, S. M., Rønnquist, A., & Labonnote, N. (2023). Fifty years of shape grammars: A systematic mapping of its application in engineering and architecture. *International Journal of Architectural Computing, 21*(1), 5-22.
25. Wei, R., & Cho, T. Y. (2021). A Study of the Influence of Shape

Grammar on Architectural Form, *Korea Institute of Design Research Society, 6*(4), 426–438.
26. Tching, J., Reis, J., & Paio, A. (2013, June). Shape grammars for creative decisions: In the architectural project. In *2013 8th Iberian Conference on Information Systems and Technologies (CISTI)* (pp. 1-6). IEEE.
27. Kobayashi, Y., Katoh, N., Okano, T., & Takizawa, A. (2015). An inductive construction of rigid panel-hinge graphs and their applications to form design. *International Journal of Architectural Computing, 13*(1), 45-63.
28. Chouchoulas, O., & Day, A. (2007). Design exploration using a shape grammar with a genetic algorithm. *open house international, 32*(2), 26-35.
29. As, I., Pal, S., & Basu, P. (2018). Artificial intelligence in architecture: Generating conceptual design via deep learning. *International Journal of Architectural Computing, 16*(4), 306-327.
30. Hillier, B., & Hanson, J. (1984). *The social logic of space*. Cambridge University Press.
31. Heitor, T., Duarte, J. P., & Pinto, R. M. (2003). Combining grammars and Space Syntax: Formulating, evaluating, and generating designs. In *Proceedings of the Fourth International Space Syntax Symposium, London: University College London* (Vol.1, pp.28.2–28.18).
32. Eloy, S., & Guerreiro, R. (2016). Transforming housing typologies. Space syntax evaluation and shape grammar generation. Transforming housing typologies. *Space syntax evaluation and shape grammar generation,* (15), 86-114.
33. Lee, J. H., Ostwald, M. J., & Gu, N. (2013). Combining space syntax and shape grammar to investigate architectural style: Considering Glenn Murcutt's domestic designs. In *Proceedings of the Ninth International Space Syntax Symposium, Seoul, Republic of Korea* (Vol. 31, pp. 5.1–5.13).
34. Lee, J. H., Ostwald, M. J., & Gu, N. (2016). A Justified Plan Graph (JPG) grammar approach to identifying spatial design patterns in an architectural style. *Environment and Planning B: Urban Analytics and City Science, 45*(1), 67-89.
35. Lee, J. H., Ostwald, M. J., & Gu, N. (2017). A Combined plan graph and massing grammar approach to frank lloyd wright's prairie architecture. *Nexus Network Journal, 19,* 279-299.
36. Cicek, S., & Turhan, G. D. (2022). Computational generation of a spatial layout through syntactical evaluation and multi-objective evolutionary optimization. *International Journal of Architectural Computing, 20*(3), 610-629.
37. Sun, M., & Meng, Q. (2022). Using spatial syntax and GIS to identify spatial heterogeneity in the main urban area of Harbin, China. *Frontiers in Earth Science, 10*, 893414.
38. Jiang, B., & Claramunt, C. (2002). Integration of space syntax into GIS: new perspectives for urban morphology. *Transactions in GIS, 6*(3), 295-309.
39. Okabe, A., Boots, B., Sugihara, K., & Chiu, S. N. (2000). Spatial tessellations: concepts and applications of Voronoi diagrams. (2nd ed.), John Willy & Sons, Chichester.
40. Feschet, F., & Lachaud, J. O. (2022, October). Full convexity for polyhedral models in digital spaces. In *International Conference on Discrete Geometry and Mathematical Morphology* (pp. 98-109). Cham: Springer International Publishing.
41. Lachaud, J. O. (2022). An alternative definition for digital convexity. *Journal of Mathematical Imaging and Vision, 64*(7), 718-735.
42. Meerpohl, C., Rick, M., & Büskens, C. (2019). Free-space polygon creation based on occupancy grid maps for trajectory optimization methods. *IFAC-PapersOnLine, 52*(8), 368-374.
43. Hector, R., Vaidyanathan, R., Sharma, G., & Trahan, J. L. (2022). Optimal convex hull formation on a grid by asynchronous robots with lights. *IEEE Transactions on Parallel and Distributed Systems, 33*(12), 3532-3545.
44. Jayaram, M. A., & Fleyeh, H. (2016). Convex hulls in image processing: a scoping review. *American Journal of Intelligent Systems, 6*(2), 48-58.
45. Franz, G., Mallot, H. A., & Wiener, J. M. (2005, August). Graph-based models of space in architecture and cognitive science: A comparative analysis. In *17th International Conference on Systems Research, Informatics and Cybernetics (INTERSYMP 2005)* (pp. 30-38). International Institute for Advanced Studies in Systems Research and Cybernetics.
46. Stiny, G., & Mitchell, W. J. (1978). The Palladian grammar, Environment and Planning B: Planning and Design.
47. Benrós, D., Duarte, J. P., & Hanna, S. (2012). A new palladian shape grammar: A subdivision grammar as alternative to the palladian grammar. *International journal of architectural computing, 10*(4), 521-540.
48. Chouchoulas, O., & Day, A. (2007). Design exploration using a shape grammar with a genetic algorithm. *open house international, 32*(2), 26-35.
49. Thaller, W., Krispel, U., Zmugg, R., Havemann, S., & Fellner, D. W. (2013). Shape grammars on convex polyhedra. *Computers & Graphics, 37*(6), 707-717.
50. Hanson, A. J. (1988). Hyperquadrics: smoothly deformable shapes with convex polyhedral bounds. *Computer vision, graphics, and image processing, 44*(2), 191-210.
51. Lee, J. H., Ostwald, M. J., & Gu, N. (2021). A statistical shape grammar approach to analysing and generating design instances of Murcutt's domestic architecture. *Environment and Planning B: Urban Analytics and City Science, 48*(4), 929-944.
52. Murray, A. T. (2021). Spatial analysis and modeling: advances and evolution. *Geographical Analysis, 53*(4), 647-664.
53. Osmond, P. (2011). The convex space as the'atom'of urban analysis. *The Journal of Space Syntax, 2*(1), 97-114.
54. Wolfram, S. (2003). *The mathematica book.* Wolfram Research, Inc..
55. *https://reference.wolfram.com/language/example/CreateAVoronoiDiagram.html* (May 7th, 2024)
56. Lynch, K. (1960). The image of the city. The MIT Press, Cambridge, MA.

Appendix of Tables

Gen.	Int.(RA)	Control
1	0.1538	0.9
2	0.1208	1.0095
3	0.1318	0.6761
4	0.0989	1.2595
5	0.1428	0.7095
6	0.1428	1.2
7	0.1758	0.6
8	0.1318	1.1261
9	0.0879	1.5
10	0.1318	1.1261
11	0.1868	0.65
12	0.1208	1.6166
13	0.2197	0.4166
14	0.1428	1.0333
15	0.1428	1.2095

Table 1: Integration and Control Measures

Gen.	Betweenness	Closeness	Degree
1	0.067155	0.535714	0.285714
2	0.065751	0.6	0.357143
3	0.019902	0.576923	0.285714
4	0.115079	0.652174	0.428571
5	0.014103	0.555556	0.285714
6	0.096459	0.555556	0.357143
7	0.018071	0.5	0.214286
8	0.059829	0.576923	0.357143
9	0.194139	0.681818	0.5
10	0.063614	0.576923	0.357143
11	0.016789	0.483871	0.214286
12	0.171062	0.6	0.428571
13	0	0.441176	0.142857
14	0.062637	0.555556	0.285714
15	0.103297	0.555556	0.357143

Table 2: Centrality Measures

Space Measurement		Clustered Generators of Roundabout Cairo														
Property	Interval	1	2	3	4	5	6	7	8	9	10	11	12	13	14	15
Control	Top-tier				x		x			x			x			x
Asymmetry	Top-tier				x					x						
Betweenness	Top-tier									x			x			
Closeness	Top-tier		x		x					x			x			
Degree	Top-tier				x					x			x			
Gabriel	4-cycles		x													
Equidistant	Nearest	x	x			x	x		x	x	x	x				
Control	Middle-high		x						x		x				x	
Asymmetry	Middle-high		x	x					x		x		x			
Betweenness	Middle-high				x		x									x
Closeness	Middle-high			x					x		x					
Degree	Middle-high		x				x		x		x					x
Gabriel	3-cycles	x		x	x					x	x					
Equidistant	Middle-high		x	x	x	x	x	x	x	x	x					
Control	Middle-low	x														
Asymmetry	Middle-low	x				x	x								x	
Betweenness	Middle-low	x	x						x		x				x	
Closeness	Middle-low	x				x	x								x	x
Degree	Middle-low	x		x		x									x	
Gabriel	2-cycles					x			x				x			
Equidistant	Middle-low	x	x	x	x			x	x	x			x			x
Control	Low			x		x		x				x		x		
Asymmetry	Low							x				x		x		
Betweenness	Low			x		x		x				x		x		
Closeness	Low							x				x		x		
Degree	Low							x				x		x		
Gabriel	1-cycle						x	x				x			x	
Gabriel	0-cycle													x		x
Equidistant	Farthest										x	x	x	x	x	x

Table 3: Concluded Cross-Correlation of Clustered Integral Properties

Appendix of Figures

Figure 1: Cairo Before Haussmann (1801). (Source: Description de L'Egypte)

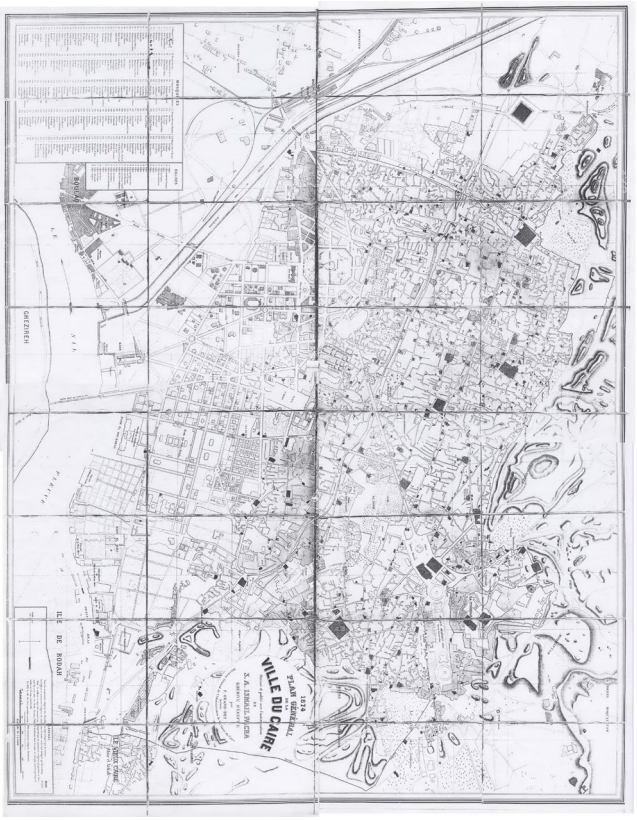

Figure 2: Cairo After Haussmann (1874). (Source: Survey Department of Egypt)

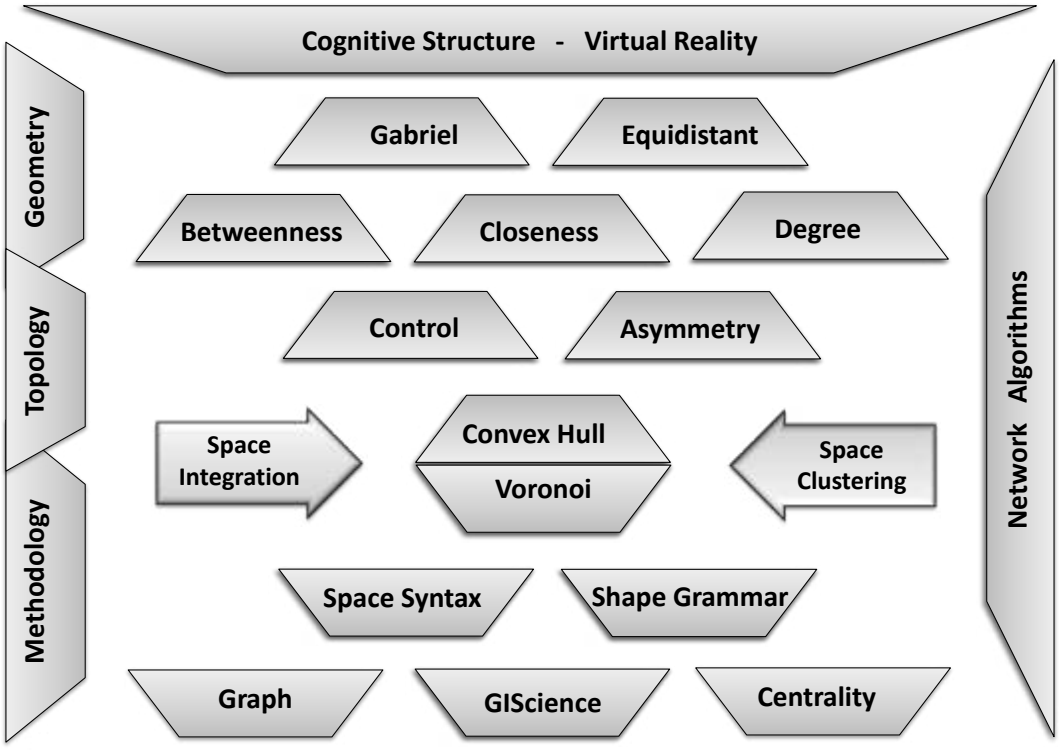

Figure 3: The Process of Voronoi Scope

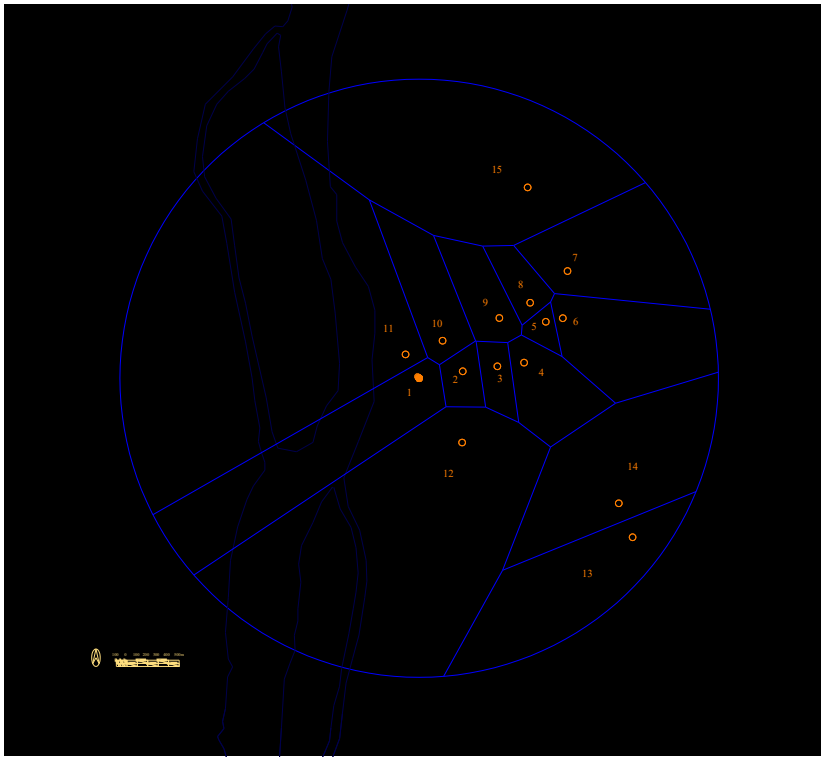

Figure 4: The Voronoi Convex Hull of Roundabout Cairo in 1867

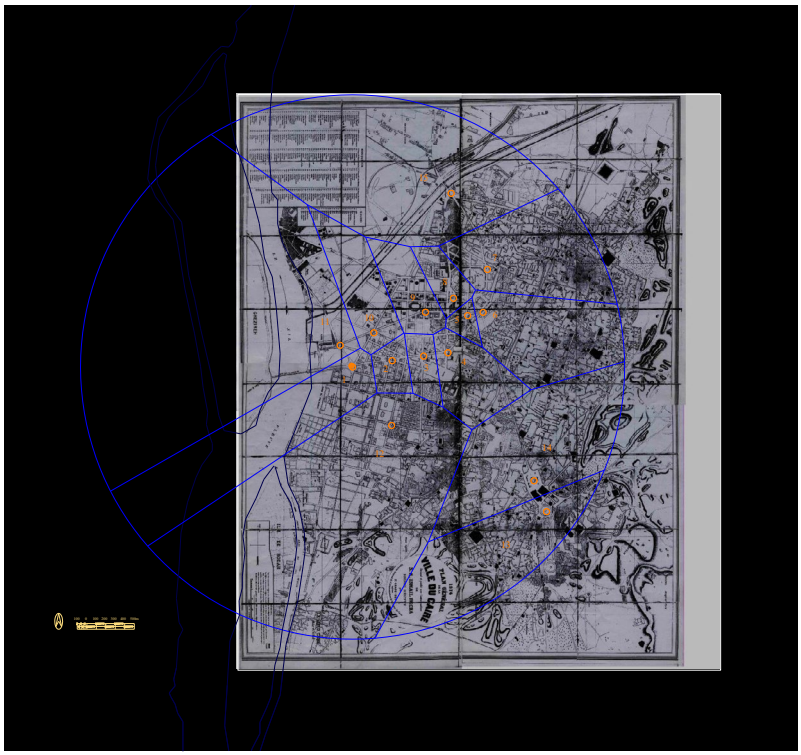

Figure 5: Overlaid Voronoi on the Map of Cairo in 1874

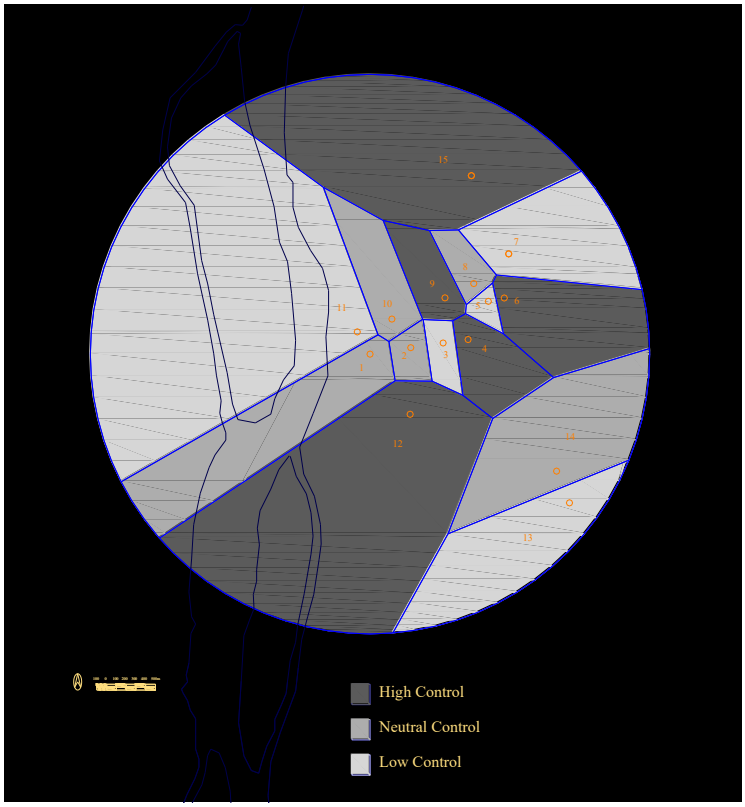

Figure 6: Spatial Control

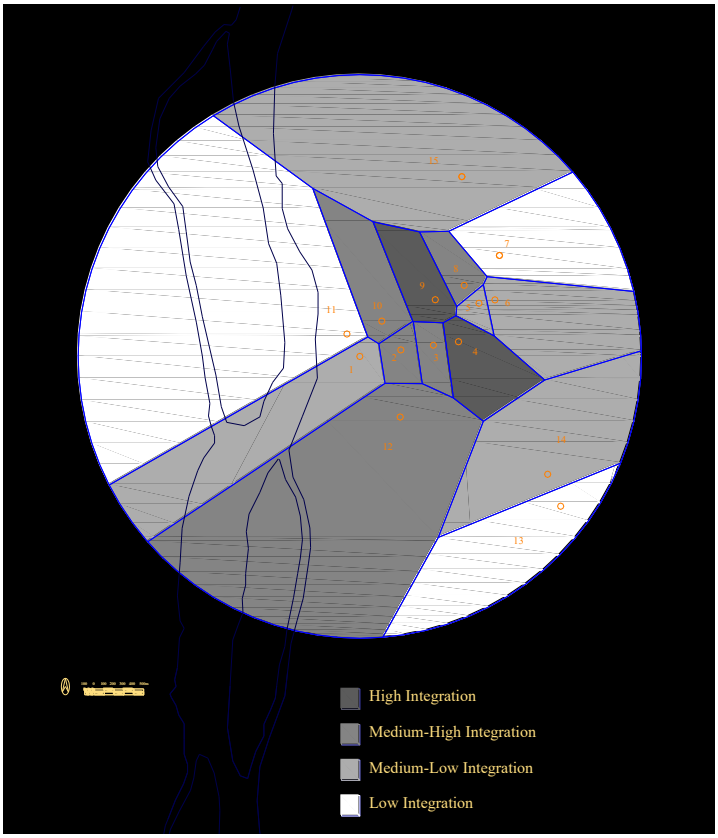

Figure 7: Spatial Integration

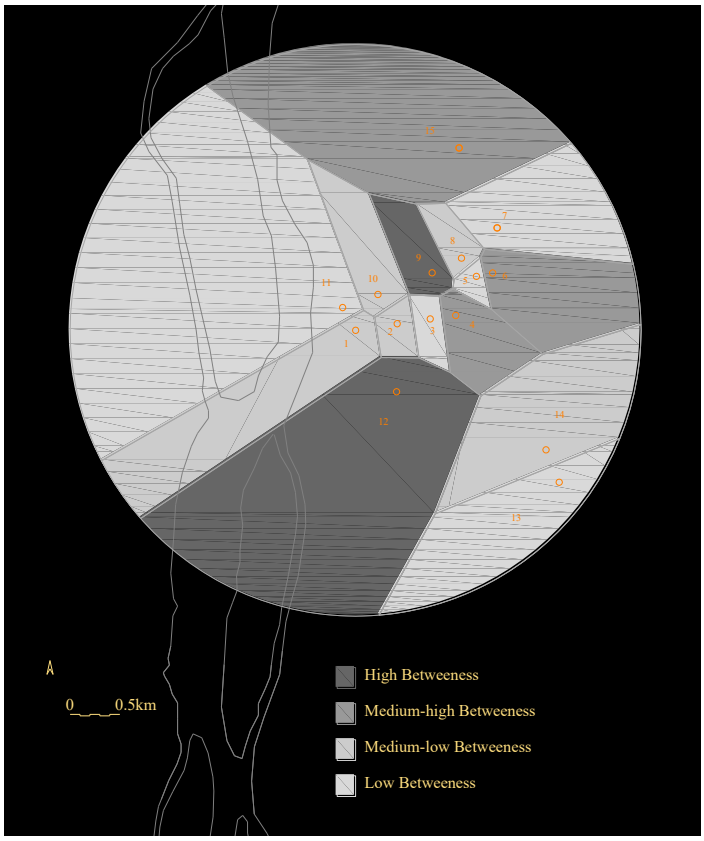

Figure 8: Spatial Betweenness

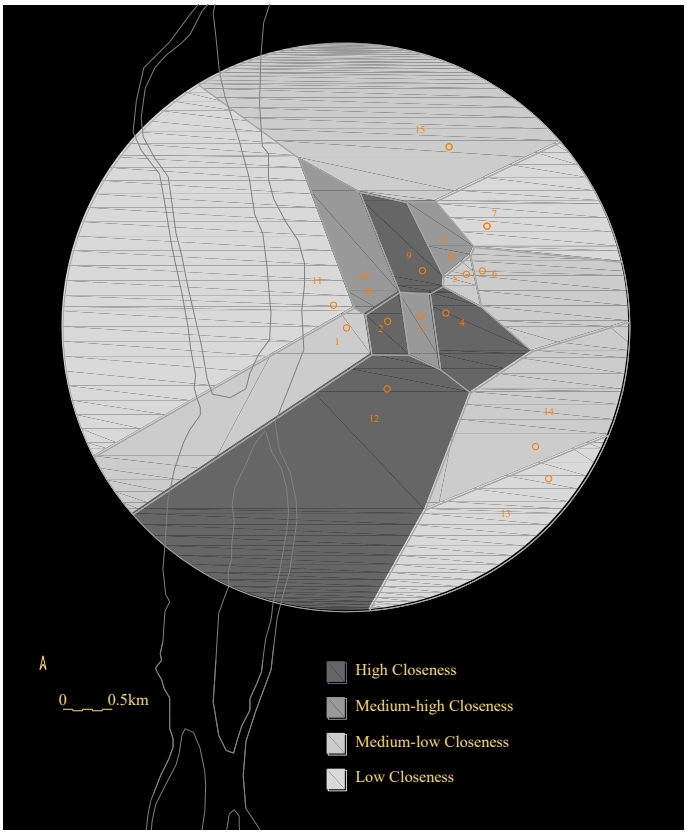

Figure 9: Spatial Closeness

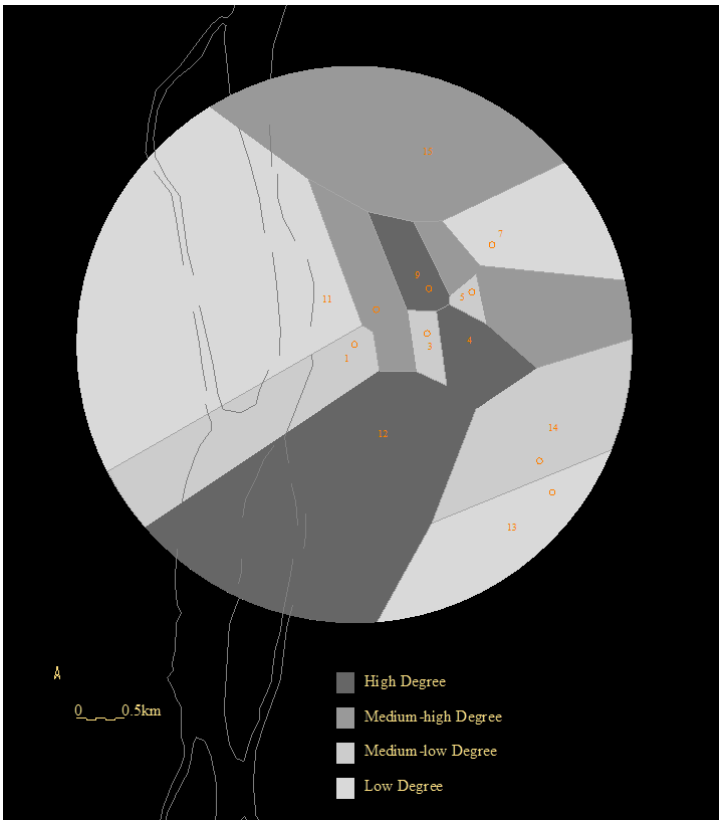

Figure 10: Spatial Degree

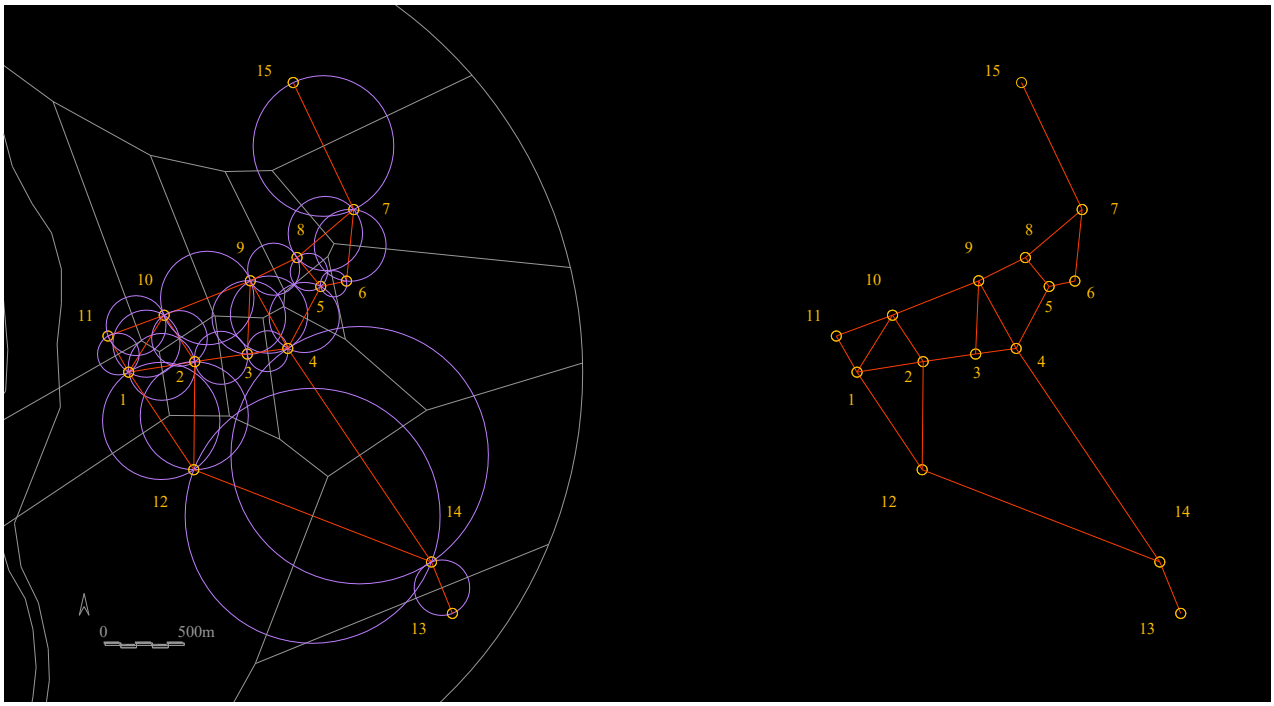

Figure 11: Gabriel Circle with Graph of Roundabout Cairo

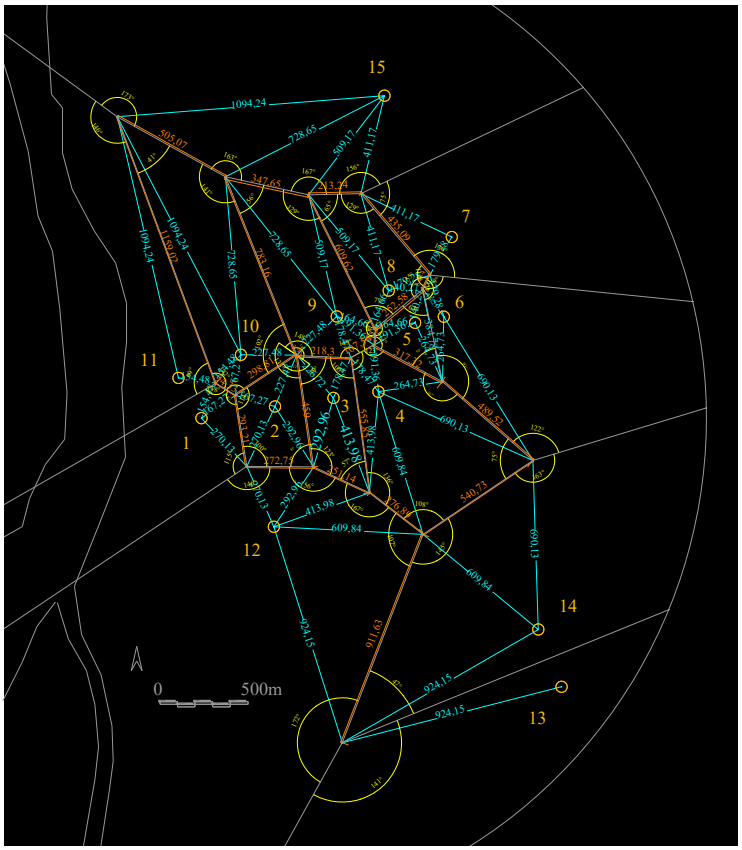

Figure 12: Equidistance of Roundabout Cairo

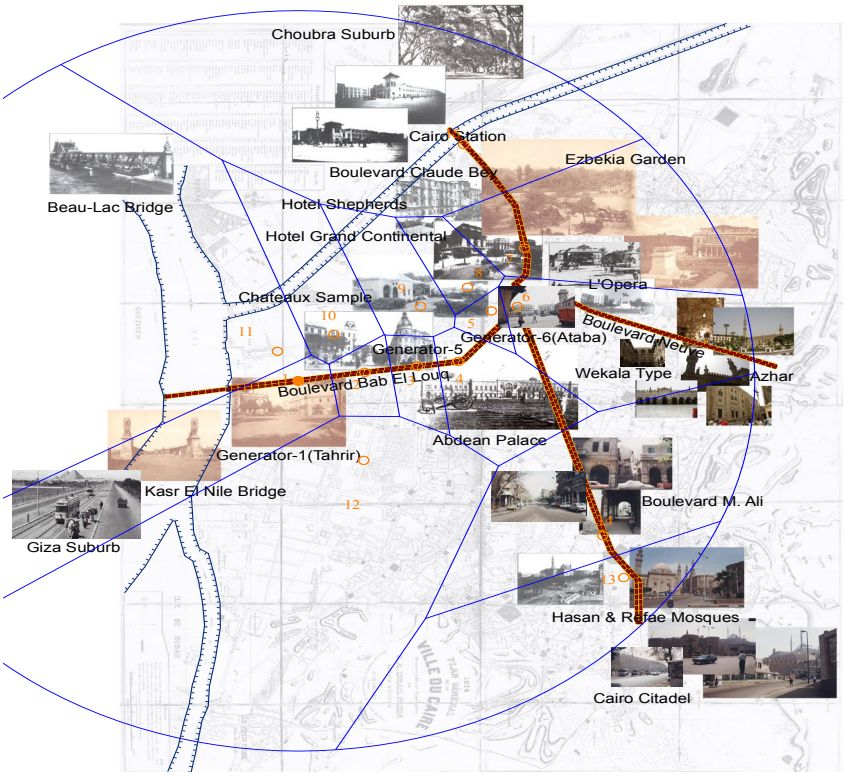

Figure 13: The Image of Voronoi Polygons

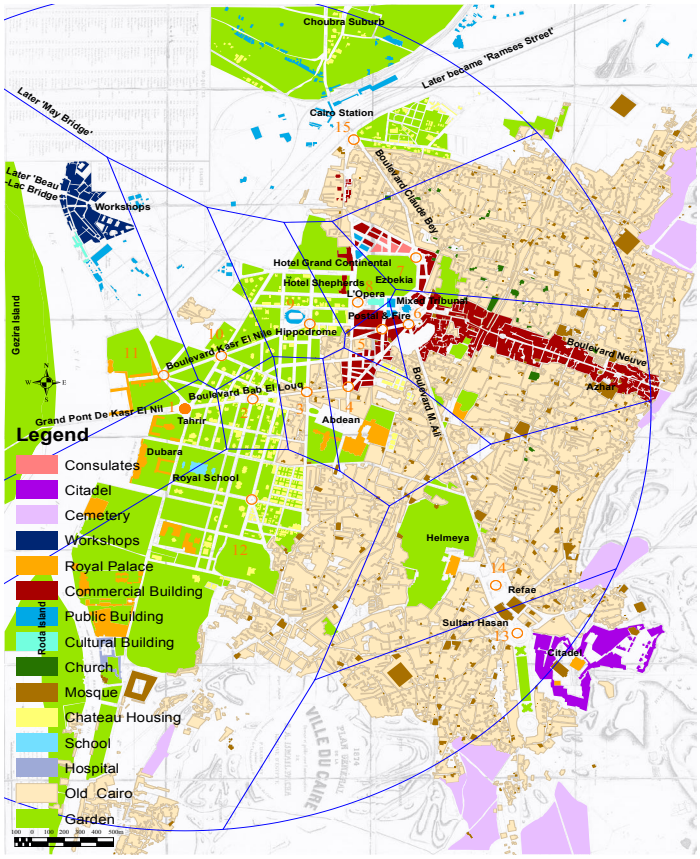

Figure 14: Function of Voronoi Polygons

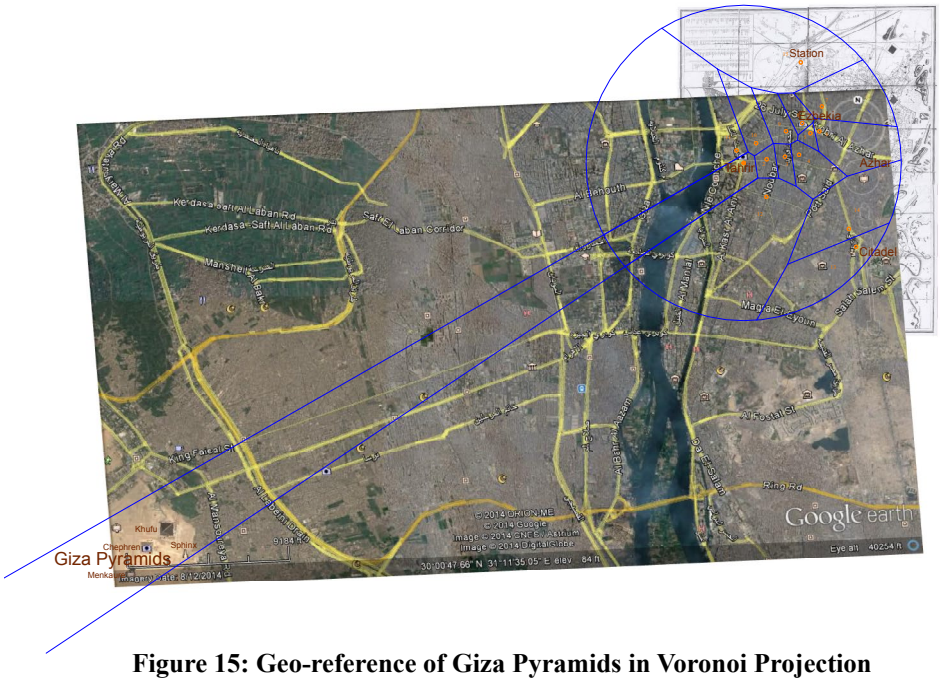

Figure 15: Geo-reference of Giza Pyramids in Voronoi Projection